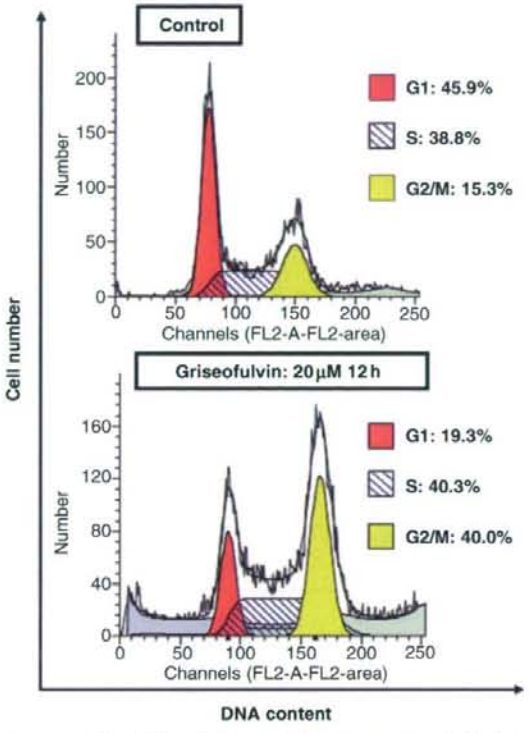

Figure 6 Griseofulvin induced G_2/M phase arrest in Huh7/Rep-Feo cells. Flow cytometry analysis of DNA content of untreated Huh7/Rep-Feo cells (control) and cells treated for 12 h with 20 μM of griseofulvin. [■ G_1: 45.9%, ▨ S: 38.8%, □ G_2/M: 15.3%; ■ G_1: 19.3%, ▨ S: 40.3%, □ G_2/M: 40.0%.]

(data not shown). The ratios of griseofulvin and IFNα were 9:1, 1:1, and 1:9. Each concentration of griseofulvin and IFNα at 50% inhibition was plotted on the X- and Y-axes, respectively, to generate an isobologram (Fig. 5b). As shown in Figure 5b, each plot fell far below the line showing additivity, indicating that the effect of the griseofulvin and IFNα combination on HCV-RNA replication is strongly synergistic.

Griseofulvin induces G_2/M cell cycle arrest in HCV replicon cells

As described previously, griseofulvin blocks cell cycle progression at the G_2/M phase in several human cell lines.[24] Here, we examined the effect of griseofulvin on cell cycle progression in Huh7/Rep-Feo cells. As shown in Figure 6, the population of griseofulvin-treated Huh7/Rep-Feo cells in the G_2/M phase at 12 h was 40%, compared to 15.3% for the control cell populations. These data imply that griseofulvin might have the potential to arrest Huh7/Rep-Feo cells in the G_2/M phase.

As described earlier, the treatment of Huh7/Rep-Feo cells with 20 μM griseofulvin for 12 h results in G_2/M arrest (Fig. 6), while treatment for 72 h had no effect on cell growth (Fig. 1c). To explain this discrepancy, we examined the growth kinetics of griseofulvin-treated Huh7/Rep-Feo cells. The cells were cultured with 20 μM griseofulvin, and cell growth was monitored by MTS assay. The cell viability declined gradually until 48 h after treatment with 20 μM griseofulvin, but increased from 48 h to 72 h (Fig. 7). These data indicate that treatment with 20 μM griseofulvin arrests Huh7/Rep-Feo cells in the G_2/M phase, but does not inhibit cell growth completely.

Griseofulvin does not inhibit HCV IRES-dependent translation

Previous studies have shown that vinblastine sulfate and nocodazole, well-characterized inhibitors of microtubule polymerization and the cell cycle in G_2/M, inhibit

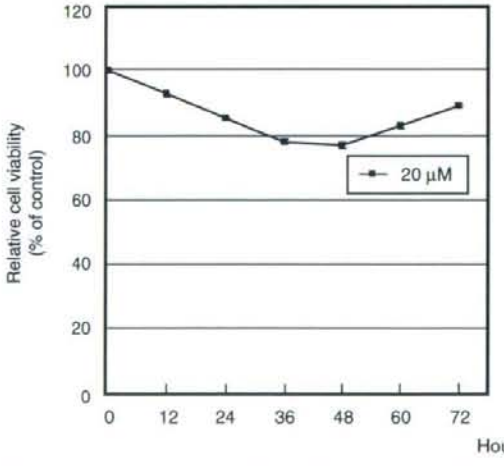

Figure 7 Growth kinetics of griseofulvin treatment of Huh7/Rep-Feo cells. Cells were cultured with [—●—] 20 μM griseofulvin, and cell viability was monitored by a 5-(3-carboxymethoxyphenyl)-2-(4,5-dimethylthiazoly)-3-(4-sulfophenyl) tetrazolium inner salt assay at the times indicated. Error bars indicate mean ± SD.

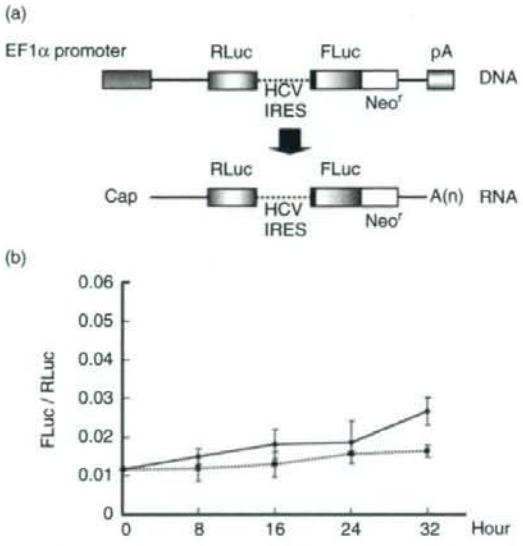

Figure 8 Griseofulvin does not influence hepatitis C virus (HCV) internal ribosomal entry site (IRES)-mediated translation. (a) Structure of the plasmid, pEF-Rluc-HCV IRES Feo. Transcription is initiated under the control of a composite elongation factor 1α (EF1α) promoter. Upstream cistron encodes Renilla luciferase (RLuc) and is translated by a cap-dependent mechanism in transfected cells, while the downstream cistron encodes a fusion (Feo) of the firefly luciferase (Fluc) and neomycin phosphotransferase (Neo') genes, translated under the control of the HCV IRES. (b) pEF-Rluc-HCV IRES Feo was stably transfected into Huh7 cells. Cells were treated without (control -◆-) and with 20 μM griseofulvin -■-. Dual luciferase activities were measured at the indicated time points after exposure to griseofulvin. Values are displayed as ratios of Fluc to Rluc. Error bars indicate mean ± SD.

HCV replication, but not HCV IRES-dependent translation.[25] Therefore, we determined whether G_2/M cell cycle arrest by griseofulvin affects HCV IRES-dependent translation using Huh7 cells transfected with pEF Rluc-HCV IRES Feo (Fig. 8a). The treatment of these cells with 20 μM griseofulvin resulted in no significant change of the internal luciferase activities, a concentration that suppressed the expression of the HCV replicon and arrested the HCV replicon cells in the G_2/M phase (Fig. 8b). These results suggested that cell cycle arrest by griseofulvin did not affect HCV IRES-dependent translation, as shown previously for vinblastine sulfate and nocodazole.

Griseofulvin suppressed JFH-1 HCV replication

The studies described thus far were carried out using the subgenomic HCV-1b replicon system. Recently, Wakita *et al.* established a cell culture model for HCV. This system, known as the JFH-1 system and based on genotype 2a HCV, allows the production of a virus that can be efficiently propagated in cell culture (HCVcc).[10] Therefore, we examined the effect of griseofulvin using the JFH-1 system. The Huh7.5.1/JFH-1 cells (cells persistently infected with HCV JFH-1) were cultured with 10 μM or 20 μM griseofulvin for 72 h. We detected the HCV NS3 protein in Huh7.5.1/JFH-1 HCV cells by immunostaining. As shown in Figure 9, in the absence of griseofulvin treatment, the NS3 protein was localized predominantly in the perinuclear region. After treatment of griseofulvin, the NS3 protein expression level was reduced substantially (Fig. 9). This result indicates that griseofulvin also suppresses HCV replication in the JFH-1 HCVcc system.

DISCUSSION

WE HAVE SHOWN here that griseofulvin inhibits the replication of HCV in the HCV subgenomic replicon cells, Huh7/Rep-Feo. In this reporter-based subgenomic replicon system, the EC_{50} of griseofulvin for the inhibition of HCV replication, determined by measurement of the luciferase activity, was approximately 6.13 μM. The real-time RT–PCR and Western blot analyses revealed that both RNA synthesis and its translation were inhibited by griseofulvin in a dose-dependent manner. The treatment of Huh7/Rep-Feo cells with griseofulvin did not activate the IFN inducible gene responses, suggesting that the inhibitory mechanism of griseofulvin in HCV replication is independent of the IFN signaling pathway. Moreover, we demonstrated that the combination treatment of griseofulvin and IFNα had a synergistic inhibitory effect in Huh7/Rep-Feo cells. We also demonstrated that griseofulvin suppressed replication of JFH-1 HCV.

A previous study demonstrated that griseofulvin induces G_2/M arrest in several human cell lines.[24] Here, we show that griseofulvin arrested the Huh7/Rep-Feo cells in the G_2/M phase. Recently, several studies have shown a correlation between HCV IRES-mediated translation and the cell cycle. Honda *et al.* reported that the HCV IRES activity was highest in the G_2/M phase.[26] In contrast, Venkatesan *et al.* reported that the HCV IRES activity was lowest in the G_2/M,[27] while other studies

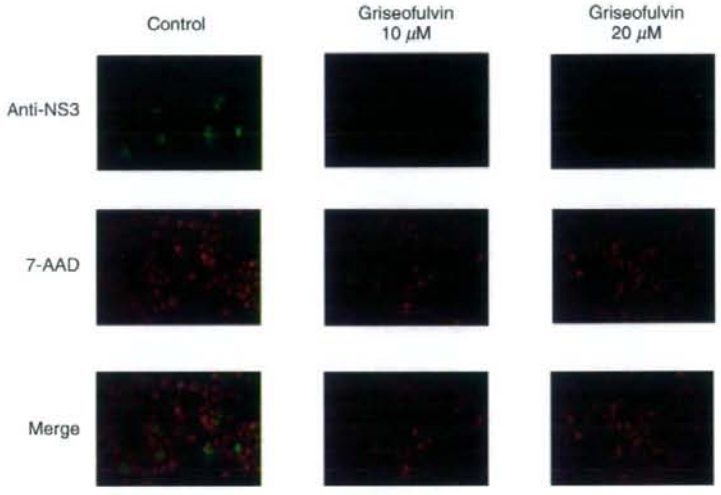

Figure 9 Griseofulvin suppresses JFH-1 replication. Immunofluorescent staining of Huh7.5.1/JFH-1 cells treated with various concentrations of griseofulvin. Hepatitis C virus NS3 protein is stained green and nuclei are stained with 7-aminoactinomycin D (7-AAD; red).

reported that the HCV IRES activity was independent of the stage of the cell cycle.[28,29] In addition, Bost *et al.* reported that several cell cycle inhibitors (vinblastine sulfate, colchicine, nocodazole, and cytochalasin D) did not affect HCV IRES-dependent translation.[25] We also have shown that cell cycle arrest by griseofulvin did not affect HCV IRES-dependent translation. Accordingly, our results support the hypothesis that the HCV IRES activity is independent of the cell cycle.

Previous studies have demonstrated that vinblastine sulfate and nocodazole, well-characterized inhibitors of microtubule polymerization, are able to inhibit HCV-RNA replication in HCV subgenomic replicon cells.[25] These findings indicate that microtubule polymerization is required for the formation of the HCV replication complex. Griseofulvin has been shown to arrest human cells in the G_2/M phase by acting on microtubule polymerization.[30] Thus it is speculated that the inhibition of microtubule polymerization by griseofulvin may influence the formation of the HCV-RNA replication complex. Further, defining the mechanism of action of griseofulvin against HCV replication may be important for defining a novel target for anti-HCV therapy.

Griseofulvin has been used for many years for the treatment of ringworm and other dermatophyte infections. Moreover, griseofulvin does not have significant toxicity for humans. Consequently, the development of derivatives of this compound may be a useful strategy for future therapeutic intervention in chronic hepatitis C.

ACKNOWLEDGMENTS

WE THANK DR Toshio Kitamura (University of Tokyo, Tokyo, Japan) for kindly providing the pGag-pol-IRES-bsr and pMXs-IN plasmids; Dr Francis V Chisari (The Scripps Research Institute, La Jolla, CA, USA) for kindly providing the Huh7.5.1 cell line; Dr Iyoko Katoh for helpful comments and discussion; and Mr Masashi Osano and Ms Ikuko Kayama (University of Yamanashi, Yamanashi, Japan) for technical assistance. This study was supported by a grant of Health Science from the Ministry of Health, Labor, and Welfare of Japan, and by a grant from the Human Sciences Foundation.

REFERENCES

1 Alter HJ, Purcell RH, Shih JW *et al.* Detection of antibody to hepatitis C virus in prospectively followed transfusion recipients with acute and chronic non-A, non-B hepatitis. *N Engl J Med* 1989; **321**: 1494–500.
2 Choo QL, Kuo G, Weiner AJ *et al.* Isolation of a cDNA clone derived from a blood-borne non-A, non-B viral hepatitis genome. *Science* 1989; **244**: 359–62.
3 Alter MJ. Epidemiology of hepatitis C. *Hepatology* 1997; **26**: 62S–5S.
4 Fried MW, Shiffman ML, Reddy KR *et al.* Peginterferon alfa-2a plus ribavirin for chronic hepatitis C virus infection. *N Engl J Med* 2002; **347**: 975–82.
5 Lohmann V, Korner F, Koch J *et al.* Replication of subgenomic hepatitis C virus RNAs in a hepatoma cell line. *Science* 1999; **285**: 110–13.

6 Kim SS, Peng LF, Lin W *et al.* A cell-based, high-throughput screen for small molecule regulators of hepatitis C virus replication. *Gastroenterology* 2007; **132**: 311–20.
7 Tanabe Y, Sakamoto N, Enomoto N *et al.* Synergistic inhibition of intracellular hepatitis C virus replication by combination of ribavirin and interferon- alpha. *J Infect Dis* 2004; **189**: 1129–39.
8 Yokota T, Sakamoto N, Enomoto N *et al.* Inhibition of intracellular hepatitis C virus replication by synthetic and vector-derived small interfering RNAs. *EMBO Rep* 2003; **4**: 602–8.
9 Lindenbach BD, Evans MJ, Syder AJ *et al.* Complete replication of hepatitis C virus in cell culture. *Science* 2005; **309**: 623–6.
10 Wakita T, Pietschmann T, Kato T *et al.* Production of infectious hepatitis C virus in tissue culture from a cloned viral genome. *Nat Med* 2005; **11**: 791–6.
11 Zhong J, Gastaminza P, Cheng G *et al.* Robust hepatitis C virus infection in vitro. *Proc Natl Acad Sci USA* 2005; **102**: 9294–9.
12 Hinrichsen H, Benhamou Y, Wedemeyer H *et al.* Short-term antiviral efficacy of BILN 2061a hepatitis C virus serine protease inhibitor, in hepatitis C genotype 1 patients. *Gastroenterology* 2004; **127**: 1347–55.
13 Lamarre D, Anderson PC, Bailey M *et al.* An NS3 protease inhibitor with antiviral effects in humans infected with hepatitis C virus. *Nature* 2003; **426**: 186–9.
14 Reesink HW, Zeuzem S, Weegink CJ *et al.* Rapid decline of viral RNA in hepatitis C patients treated with VX-950: a phase Ib, placebo-controlled, randomized study. *Gastroenterology* 2006; **131**: 997–1002.
15 Sarrazin C, Rouzier R, Wagner F *et al.* SCH 503034, a novel hepatitis C virus protease inhibitor, plus pegylated interferon alpha-2b for genotype 1 nonresponders. *Gastroenterology* 2007; **132**: 1270–8.
16 Amemiya F, Maekawa S, Itakura Y *et al.* Targeting lipid metabolism in the treatment of hepatitis C. *J Infect Dis* 2008; **197**: 361–70.
17 Martell M, Gomez J, Esteban JI *et al.* High-throughput real-time reverse transcription-PCR quantitation of hepatitis C virus RNA. *J Clin Microbiol* 1999; **37**: 327–32.
18 Okada Y, Osada M, Kurata S *et al.* p53 gene family p51 (p63) -encoded, secondary transactivator p51B (TAp63alpha) occurs without forming an immunoprecipitable complex with MDM2, but responds to genotoxic stress by accumulation. *Exp Cell Res* 2002; **276**: 194–200.
19 Chou TC, Talaly P. A simple generalized equation for the analysis of multiple inhibitions of Michaelis–Menten kinetic systems. *J Biol Chem* 1977; **252**: 6438–42.
20 Kitamura T, Koshino Y, Shibata F *et al.* Retrovirus-mediated gene transfer and expression cloning: powerful tools in functional genomics. *Exp Hematol* 2003; **31**: 1007–14.
21 Morita S, Kojima T, Kitamura T. Plat-E: an efficient and stable system for transient packaging of retroviruses. *Gene Ther* 2000; **7**: 1063–6.
22 Blight KJ, Kolykhalov AA, Rice CM. Efficient initiation of HCV RNA replication in cell culture. *Science* 2000; **290**: 1972–4.
23 Frese M, Pietschmann T, Moradpour D *et al.* Interferon-alpha inhibits hepatitis C virus subgenomic RNA replication by an MxA-independent pathway. *J Gen Virol* 2001; **82**: 723–3.
24 Ho YS, Duh JS, Jeng JH *et al.* Griseofulvin potentiates antitumorigenesis effects of nocodazole through induction of apoptosis and G2/M cell cycle arrest in human colorectal cancer cells. *Int J Cancer* 2001; **91**: 393–401.
25 Bost AG, Venable D, Liu L *et al.* Cytoskeletal requirements for hepatitis C virus (HCV) RNA synthesis in the HCV replicon cell culture system. *J Virol* 2003; **77**: 4401–8.
26 Honda M, Kaneko S, Matsushita E *et al.* Cell cycle regulation of hepatitis C virus internal ribosomal entry site-directed translation. *Gastroenterology* 2000; **118**: 152–62.
27 Venkatesan A, Sharma R, Dasgupta A. Cell cycle regulation of hepatitis C and encephalomyocarditis virus internal ribosome entry site-mediated translation in human embryonic kidney 293 cells. *Virus Res* 2003; **94**: 85–95.
28 Nelson HB, Tang H. Effect of cell growth on hepatitis C virus (HCV) replication and a mechanism of cell confluence-based inhibition of HCV RNA and protein expression. *J Virol* 2006; **80**: 1181–90.
29 Scholle F, Li K, Bodola F, Ikeda M *et al.* Virus–host cell interactions during hepatitis C virus RNA replication: impact of polyprotein expression on the cellular transcriptome and cell cycle association with viral RNA synthesis. *J Virol* 2004; **78**: 1513–24.
30 Panda D, Rathinasamy K, Santra MK *et al.* Kinetic suppression of microtubule dynamic instability by griseofulvin: implications for its possible use in the treatment of cancer. *Proc Natl Acad Sci USA* 2005; **102**: 9878–83.

doi:10.1111/j.1440-1746.2007.05076.x

HEPATOLOGY

Inhibition of hepatitis C virus infection and expression *in vitro* and *in vivo* by recombinant adenovirus expressing short hairpin RNA

Naoya Sakamoto,*,† Yoko Tanabe,* Takanori Yokota,‡ Kenichi Satoh,§ Yuko Sekine-Osajima,* Mina Nakagawa,*,† Yasuhiro Itsui,* Megumi Tasaka,* Yuki Sakurai,* Chen Cheng-Hsin,* Masahiko Yano,¶ Shogo Ohkoshi,¶ Yutaka Aoyagi,¶ Shinya Maekawa,†† Nobuyuki Enomoto,†† Michinori Kohara§ and Mamoru Watanabe*

Departments of *Gastroenterology and Hepatology, †Hepatitis Control, and ‡Neurology and Neurological Science, Tokyo Medical and Dental University, §Department of Microbiology and Cell Biology, The Tokyo Metropolitan Institute of Medical Science, Tokyo, ¶Gastroenterology and Hepatology Division, Graduate School of Medical and Dental Sciences, Niigata University, Niigata, and ††First Department of Medicine, Yamanashi University, Yamanashi, Japan

Key words
adenovirus vector, hepatitis C virus, RNA interference.

Accepted for publication 12 April 2007.

Correspondence
Dr Naoya Sakamoto, Department of Gastroenterology and Hepatology, Tokyo Medical and Dental University, 1-5-45 Yushima, Bunkyo-ku, Tokyo 113-8519, Japan.
Email: nsakamoto.gast@tmd.ac.jp

NS and YT have contributed equally to this paper.

Abstract

Background and Aim: We have reported previously that synthetic small interfering RNA (siRNA) and DNA-based siRNA expression vectors efficiently and specifically suppress hepatitis C virus (HCV) replication *in vitro*. In this study, we investigated the effects of the siRNA targeting HCV-RNA *in vivo*.

Methods: We constructed recombinant retrovirus and adenovirus expressing short hairpin RNA (shRNA), and transfected into replicon-expressing cells *in vitro* and transgenic mice *in vivo*.

Results: Retroviral transduction of Huh7 cells to express shRNA and subsequent transfection of an HCV replicon into the cells showed that the cells had acquired resistance to HCV replication. Infection of cells expressing the HCV replicon with an adenovirus expressing shRNA resulted in efficient vector delivery and expression of shRNA, leading to suppression of the replicon in the cells by ~10^{-3}. Intravenous delivery of the adenovirus expressing shRNA into transgenic mice that can be induced to express HCV structural proteins by the Cre/*lox*P switching system resulted in specific suppression of virus protein synthesis in the liver.

Conclusion: Taken together, our results support the feasibility of utilizing gene targeting therapy based on siRNA and/or shRNA expression to counteract HCV replication, which might prove valuable in the treatment of hepatitis C.

Introduction

Hepatitis C virus (HCV), which affects 170 million people worldwide, is one of the most important pathogens causing liver-related morbidity and mortality.[1] The difficulty in eradicating HCV is attributable to limited treatment options against the virus and their unsatisfactory efficacies. Even with the most effective regimen with pegylated interferon (IFN) and ribavirin in combination, the efficacies are limited to less than half of the patients treated.[2] Given this situation, the development of safe and effective anti-HCV therapies is one of our high-priority goals.

RNA interference (RNAi) is a process of sequence-specific, post-transcriptional gene silencing that is initiated by double-stranded RNA.[3,4] Because of its potency and specificity, RNAi rapidly has become a powerful tool for basic research to analyze gene functions and for potential therapeutic applications. Recently, successful suppression of various human pathogens by RNAi have been reported, including human immunodeficiency viruses,[5,6] poliovirus,[7] influenza virus,[8] severe acute respiratory syndrome (SARS) virus[9] and hepatitis B virus (HBV).[10-13]

We and other researchers have reported that appropriately designed small interfering RNA (siRNA) targeting HCV genomic RNA can efficiently and specifically suppress HCV replication *in vitro*.[14-19] We have tested siRNA designed to target the well-conserved 5′-untranslated region (5′-UTR) of HCV-RNA, and identified the most effective target, just upstream of the translation initiation codon. Furthermore, transfection of DNA-based vectors expressing siRNA was as effective as that of synthetic siRNA in suppressing HCV replication.[14]

In this study, we explored the further possibility that efficient delivery and expression of siRNA may be effective in suppression and elimination of HCV replication and that delivery of such

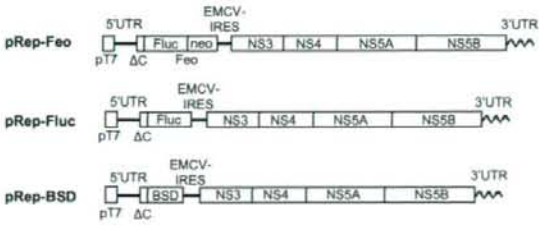

Figure 1 Structures of HCV replicon plasmids. The pRep-Feo expressed a chimeric reporter protein of firefly luciferase (Fluc) and neomycin phosphotransferase (GenBank accession No. AB119282).[14,20] The pRep-Fluc expressed the Fluc protein. The pRep-BSD expressed the blasticidin S (BSD) resistance gene. pT7, T7 promoter; 5'UTR, HCV 5'-untranslated region; ΔC, truncated HCV core region (nt. 342–377); neo, neomycin phosphotransferase gene; EMCV, encephalomyocarditis virus; NS3, NS4, NS5A and NS5B, genes that encode HCV non-structural proteins; 3'UTR, HCV 3'-untranslated region.

HCV-directed siRNA *in vivo* may be effective in silencing viral protein expression in the liver. Here, we report that HCV replication was suppressed *in vitro* by recombinant retrovirus and adenovirus vectors expressing short hairpin RNA (shRNA) and that the delivery of the adenovirus vector to mice *in vivo* specifically inhibited viral protein synthesis in the liver.

Methods

Cells and cell culture

Huh7 and Retro Pack PT67 cells (Clontech, Palo Alto, CA, USA) were maintained in Dulbecco's modified minimal essential medium (Sigma, St. Louis, MO, USA) supplemented with 10% fetal calf serum at 37°C under 5% CO_2. To maintain cell lines carrying the HCV replicon, G418 (Wako, Osaka, Japan) was added to the culture medium to a final concentration of 500 μg/mL.

HCV replicon constructs and transfection

HCV replicon plasmids, pRep-Feo, pRep-Fluc and pRep-BSD were constructed from were constructed from a virus, HCV-N strain, genotype 1b.[21] The pRep-Feo expressed a chimeric reporter protein of firefly luciferase (Fluc) and neomycin phosphotransferase.[14,20] The pRep-Fluc and the pRep-BSD expressed the Fluc and blasticidin S (BSD) resistance genes, respectively (Fig. 1). The replicon RNA synthesis and the transfection protocol have been described previously.[22]

Synthetic siRNA and siRNA-expression plasmid

The design and construction of HCV-directed siRNA vectors have been described.[14] Briefly, five siRNA targeting the 5'-UTR of HCV RNA were tested for their efficiency to inhibit HCV replication, and the most effective sequence, which targeted nucleotide position of 331 though 351, was used in the present study. To construct shRNA-expressing DNA cassettes, oligonucleotide inserts were synthesized that contained the loop sequence (5'-TTC AAG AGA-3') flanked by sense and antisense siRNA sequences (Fig. 2a). These were inserted immediately downstream of the human U6 promoter. To avoid a problem in transcribing shRNA because of instability of the DNA strands arising from the tight palindrome structure, several C-to-T point mutations, which retained completely the silencing activity of the shRNA, were introduced into the sense strand of the shRNA sequences (referred to as 'm').[23] A control plasmid, pUC19-shRNA-Control, expressed shRNA directed towards the Machado–Joseph disease gene, which is a mutant of ataxin-3 gene and is not normally expressed. We have previously described the sequence specific activity of the shRNA-Control.[24]

Prior to construction of the virus vectors, we tested silencing efficiency of five shRNA constructs of different lengths that covered the target sequence (Fig. 2a). The shRNA-HCV-19, shRNA-HCV-21 and shRNA-HCV-27 had target sequences of 19, 21 and 27 nucleotides, respectively. Transfection of these shRNA constructs into Huh7/pRep-Feo showed that shRNA with longer target sequences had better suppressive effects (Fig. 2b). Therefore, we used shRNA-HCV-27m (abbreviated as shRNA-HCV) in the following study.

Recombinant retrovirus vectors

The U6-shRNA expression cassettes were inserted into the *StuI*/*Hin*dIII site of a retrovirus vector, pLNCX2 (Clontech) to construct pLNCshRNA-HCV and pLNCshRNA-Control (Fig. 2c). The plasmids were transfected into the packaging cells, Retro Pack PT67. The culture supernatant was filtered and added onto Huh7 cells with 4 μg/mL of polybrene. Huh7 cell lines stably expressing shRNA were established by culture in the presence of 500 μg/mL of G418.

Recombinant adenovirus

Recombinant adenoviruses expressing shRNA were constructed using an Adenovirus Expression Vector Kit (Takara, Otsu, Japan). The U6-shRNA expression DNA cassette was inserted into the *SwaI* site of pAxcw to construct pAxshRNA-HCV and pAxshRNA-Control. The adenoviruses were propagated according to the manufacturer's protocol (AxshRNA-HCV and AxshRNA-Control; Fig. 2c). A 'multiplicity of infection' (MOI) was used to standardize infecting doses of adenovirus. The MOI stands for the ratio of infectious virus particles to the number of cells being infected. An MOI = 1 represents equivalent dose to introduce one infectious virus particle to every host cell that is present in the culture.

Plasmids for assays of interferon responses

pISRE-TA-Luc (Invitrogen, Carlsbad, CA, USA) contained five copies of the consensus interferon stimulated response element (ISRE) motifs upstream of the Fluc gene. pTA-Luc (Invitrogen), which lacks the enhancer element, was used for background determination. The pcDNA3.1 (Invitrogen) was used as an empty vector for mock transfection. pRL-CMV (Promega, Madison, WI, USA), which expresses the *Renilla* luciferase protein, was used for normalization of transfection efficiency.[25] A plasmid, peGFPneo (Invitrogen), was used to monitor percentages of transduced cells.

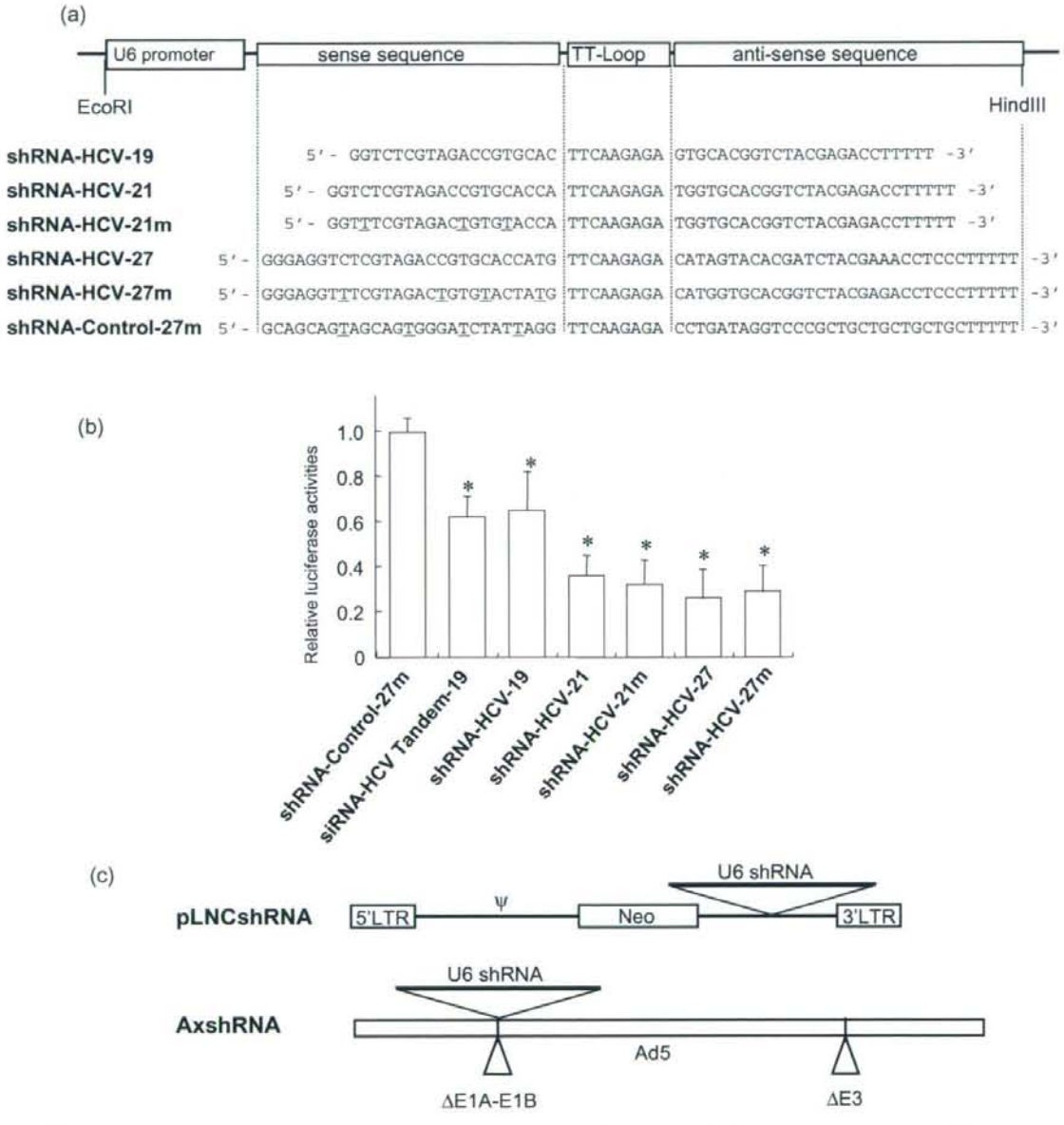

Figure 2 Structure of shRNA-expression constructs and shRNA sequences. (a) Structure of shRNA-expression cassette and shRNA sequences. TT-Loop, the loop sequence. The shRNA-Control was directed toward an unrelated target, Machado–Joseph disease gene. Underlined letters indicate C-to-T point mutations in the sense strand. (b) The shRNA-expression plasmids were transfected into Huh7/pRep-Feo cells, and internal luciferase activities were measured at 48 h of transfection. Each assay was done in triplicate, and the values are displayed as mean + SD. $^*P < 0.05$. (c) pLNCshRNA, structure of a recombinant retrovirus expressing shRNA. Ψ, the retroviral packaging signal sequence. AxshRNA, structure of a recombinant adenovirus expressing shRNA.

Real-time RT-PCR analysis

Total cellular RNA was extracted from cultured cells or liver tissue using ISOGEN (Nippon Gene, Tokyo, Japan). Total cellular RNA (2 μg) was used to generate cDNA from each sample using the SuperScript II reverse-transcriptase (Invitrogen). The mRNA expression levels were measured using the Light Cycler PCR and detection system (Roche, Mannheim, Germany) and Light Cycler Fast Start DNA Master SYBR Green 1 mix (Roche).

Luciferase assays

Luciferase activity was measured using a luminometer, Lumat LB9501 (Promega) and the Bright-Glo Luciferase Assay System (Promega) or the Dual-Luciferase Reporter Assay System (Promega).

Northern and western hybridization

Total cellular RNA was separated by denaturing agarose-formaldehyde gel electrophoresis, and transferred to a nylon membrane. The membrane was hybridized with a digoxigenin-labeled probe specific for the full-length replicon sequence, and subsequently with a probe specific for beta-actin. The signals were detected by chemiluminescence reaction using a Digoxigenin Luminescent Detection Kit (Roche), and visualized by Fluoro-Imager (Roche). For the western blotting, 10 μg of total cell lysate was separated on NuPAGE 4.12% Bis-TrisGel (Invitrogen), and blotted onto an Immobilon PVDF Membrane (Roche). The membrane was incubated with monoclonal antibodies specific for HCV-NS5A (BioDesign, Saco, ME, USA), NS4A (Virogen, Watertown, MA, USA), or beta-actin (Sigma), and detected by a chemiluminescence reaction (BM Chemiluminescence Blotting Substrate; POD, Roche).

Transient-replication assays

A replicon, pRep-Fluc, was transfected into cells and the luciferase activities of the cell lysates were measured serially. To correct the transfection efficiency, each value was divided by the luciferase activity at 4 h after the transfection.

Stable colony formation assays

Cells were transfected with a replicon, pRep-BSD, and were cultured in the presence of 150 μg/mL of BSD (Invitrogen). BSD-resistant cell colonies appeared after ~3 weeks of culture, and were counted.

HCV-JFH1 virus cell culture

An *in-vitro* transcribed HCV-JFH1 RNA[26] was transfected into Huh7.5.1 cells.[27] Naive Huh7.5.1 cells were subsequently infected by the culture supernatant of the JFH1-RNA transfected Huh-7.5.1 cells, and subjected to siRNA or drug treatments. Replication levels of HCV-RNA were quantified by the realtime RT-PCR by using primers that targeted HCV-NS5B region, HCV-JFH1 sense: 5′-TCA GAC AGA GCC TGA GTC CA-3′, and HCV-JFH1 antisense: 5′-AGT TGC TGG AGG GCT TCT GA-3′.

Mice and adenovirus infection

Transgenic mice, CN2-29, inducibly express mRNA for the HCV structural proteins (genotype1b, nucleotides 294–3435) by the Cre/*lox*P switching system.[28] The transgene does not contain full-length HCV 5′-UTR, but shares the target sequence of the shRNA-HCV. Although the transgenic mouse CN2 has been previously reported as expressing higher levels of the viral proteins, the expression levels of the viral core protein in the CN2-29 mice are modest and similar to that in the liver of HCV patients. Thus, we chose CN2-29 mice in the present study.

The mice were infected with AxshRNA-HCV or controls (AxshRNA-Control or AxCAw1) in combination with AxCAN-Cre, which expressed Cre recombinase. Three days after the infection, the mice were killed and HCV core protein in the liver was measured as described below. The BALB/c mice were maintained in the Animal Care Facility of Tokyo Medial and Dental University, and transgenic mice were in the Tokyo Metropolitan Institute of Medical Science. Animal care was in accordance with institutional guidelines. The review board of the university approved our experimental animal studies and all experiments were approved by the institutional animal study committees.

Measurement of HCV core protein in mouse liver

The amounts of HCV core protein in the liver tissue from the mice was measured by a fluorescence enzyme immunoassay (FEIA)[29] with a slight modification. Briefly, the 5F11 monoclonal anti-HCV-core antibody was used as the first antibody on the solid phase, and the 5E3 antibody conjugated with horseradish peroxidase was the second antibody. This FEIA can detect as little as 4 pg/mL of recombinant HCV-core protein. Contents of the HCV core protein in the liver samples were normalized by the total protein contents and expressed as pg/mg total protein.

Immunohistochemical staining

Liver tissue was frozen with optimal cutting temperature (OTC) compound (Tissue Tek; Sakura Finetechnical, Tokyo, Japan). The sections (8 μm thick) were fixed with a 1:1 solution of acetone : methanol at −20°C for 10 min and then washed with phosphate-buffered saline (PBS). Subsequently, the sections were incubated with the IgG fraction of an anti-HCV core rabbit polyclonal antibody (RR8)[28] in blocking buffer or antialbumin rabbit polyclonal antibody (Dako Cytomation, Glostrup, Denmark) in PBS overnight at 4°C. The sections were incubated with secondary antibody, Alexa-antirabbit IgG (Invitrogen) or TRITIC-antirabbit IgG (Sigma), for 2 h at room temperature. Fluorescence was observed using a fluorescence microscope.

Statistical analyses

Statistical analyses were performed using Student's *t*-test; *P*-values of less than 0.05 were considered to be statistically significant.

Results

Retrovirus transduction of shRNA can protect from HCV replication

Retrovirus vectors propagated from pLNCshRNA-HCV and pLNCshRNA-Control were used to infect Huh7 cells, and cell lines were established that constitutively express shRNA-HCV and shRNA-Control (Huh7/shRNA-HCV and Huh7/shRNA-Control, respectively). There were no differences in the cell morphology or growth rate between shRNA-transduced and non-transduced Huh7 cells (data not shown). The HCV replicon, pRep-Fluc, was transfected into Huh7/shRNA-HCV, Huh7/shRNA-Control and naive Huh7 cells by electroporation. In Huh7/shRNA-Control and naive Huh7 cells, the initial luciferase activity at 4 h decreased temporarily, which represents decay of the transfected replicon RNA, but increased again at 48 h and 72 h, which demonstrate de novo synthesis of the HCV replicon RNA. In contrast, transfection into Huh7/shRNA-HCV cells resulted in a decrease in the initial luciferase activity, reaching background by 72 h (Fig. 3a). Similarly, transfection of the replicon, pRep-BSD, into Huh7 cells and BSD selection yielded numerous BSD-resistant colonies in the naive Huh7 (832 colonies) and Huh7/shRNA-Control cell lines (740 colonies), while transfection of Huh7/shRNA-HCV, which expressed shRNA-HCV, yielded obviously fewer colonies (five colonies), indicating reduction of colony forming units by ~10^2 (Fig. 3b). There was no difference in shape, growth or viability between cells expressing the shRNA or not. These results indicated that cells expressing HCV-directed shRNA following retrovirus transduction acquired resistance to HCV replication.

Effect of recombinant adenoviruses expressing shRNA on *in vitro* HCV replication

We investigated subsequently the effects of recombinant adenovirus vectors expressing shRNA. AxshRNA-HCV and AxshRNA-Control were used separately to infect Huh7/pRep-Feo cells, and the internal luciferase activities were measured sequentially (Fig. 4a). AxshRNA-HCV caused continuous suppression of HCV RNA replication. Six days postinfection, the luciferase activities fell to background levels. In contrast, the luciferase activities of the Huh7/pRep-Feo cells infected with AxshRNA-Control did not show any significant changes compared with untreated Huh7/pRep-Feo cells (Fig. 4a). The dimethylthiazol carboxymethoxyphenyl sulfophenyl tetrazolium (MTS) assay showed no significant difference between cells that were infected by recombinant adenovirus and uninfected cells (Fig. 4b). In the northern blotting analysis, the cells were harvested 6 days after infection with the adenovirus at an MOI of 1. Feo-replicon RNA of 9.6 kb, which was detectable in the untreated Huh7/pRep-Feo cells and in the cells infected with AxshRNA-Control, diminished substantially following infection with the AxshRNA-HCV (Fig. 4c). Densitometries showed that the intracellular levels of the replicon RNA in the Huh7/pRep-Feo cells correlated well with the internal luciferase activities. Similarly in the western blotting, cells were harvested 6 days after infection with adenovirus. Levels of the HCV NS4A and NS5A proteins that were translated from the HCV replicon decreased following infection with the AxshRNA-HCV

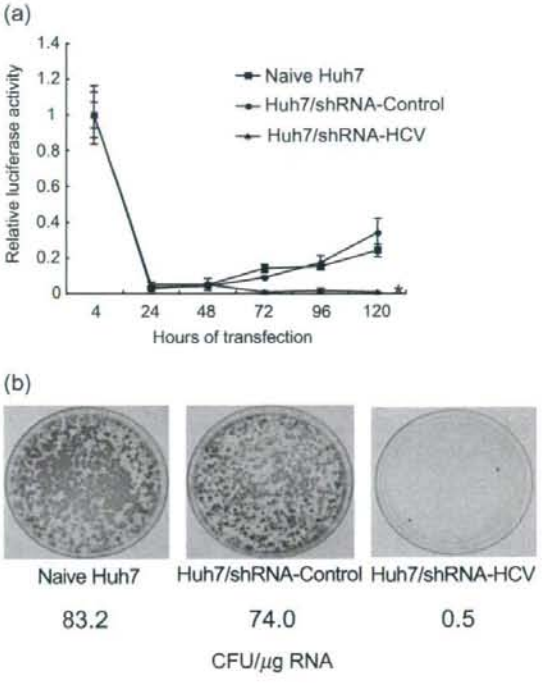

Figure 3 HCV replication can be inhibited by shRNA-HCV which was stably transfected into cells. Huh7/shRNA-HCV and Huh7/shRNA-Control stably express shRNA-HCV or shRNA-Control, respectively, following retroviral transduction. (a) Transient replication assay. An HCV replicon RNA, pRep-Fluc, was transfected into naive Huh7, Huh7/shRNA-HCV and Huh7/shRNA-Control cells. Luciferase activities of the cell lysates were measured serially at the times indicated, and the values were plotted as ratios relative to luciferase activities at 4 h. The luciferase activities at 4 h represent transfected replicon RNA. The data are mean ± SD. An asterisk denotes a *P*-value of less than 0.001 compared with the corresponding value of the naive Huh7 cells. (b) Stable colony formation assay. The HCV replicon, pRep-BSD, was transfected into naive Huh7, Huh7/shRNA-HCV and Huh7/shRNA-Control cells. The cells were cultured in the presence of blasticidin S (BSD) in the medium for ~3 weeks, and the BSD-resistant colonies were counted. These assays were repeated twice. The colony-forming units per microgram RNA (CFU/μg RNA) are shown at the bottom.

(Fig. 4d). These results indicated that the decrease in luciferase activities was due to specific suppressive effects of shRNA on expression of HCV genomic RNA and the viral proteins, and not due to non-specific effects caused by the delivery of shRNA or to toxicity of the adenovirus vectors.

Absence of interferon-stimulated gene responses by siRNA delivery

It has been reported that double-stranded RNA may induce interferon-stimulated gene (ISG) responses which cause instability of mRNA, translational suppression of proteins and apoptotic cell

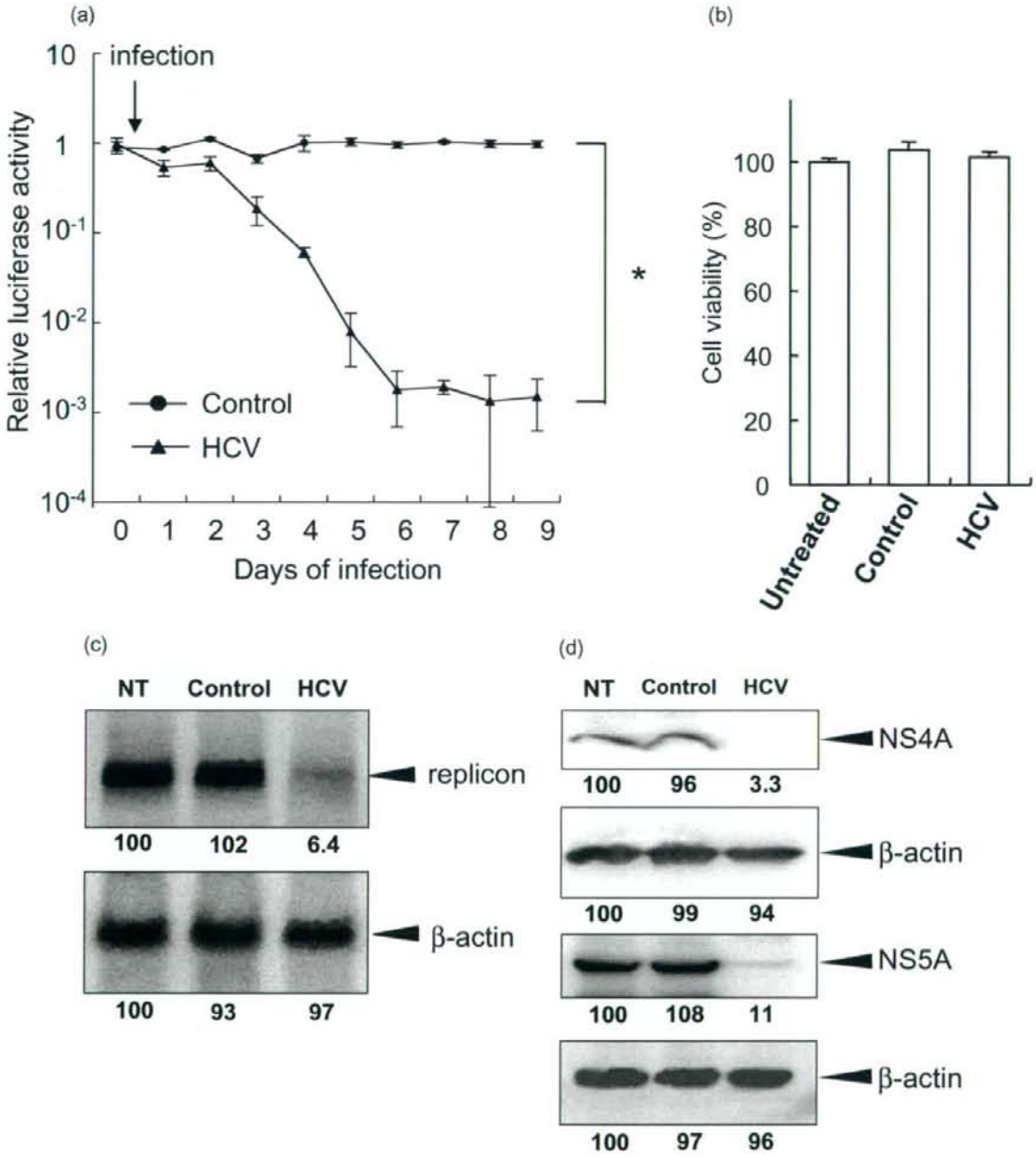

death.[18,30,31] Therefore, we examined the effects of the shRNA-expressing plasmids and adenoviruses on the activation of ISG expression in cells. The ISRE-reporter plasmid, pISRE-TA-Luc, and a control plasmid, peGFPneo, were transfected into Huh7 cells with plasmid pUC19-shRNA-HCV or pUC19-shRNA-Control, or adenovirus, AxshRNA-HCV or AxshRNA-Control, and the ISRE-mediated luciferase activities were measured. On day 2, the ISRE-luciferase activities did not significantly change in cells in which

Figure 4 Effect of a recombinant adenovirus expressing shRNA on HCV replicon. (a) Huh7/pRep-Feo cells were infected with AxshRNA-HCV or shRNA-Control at a multiplicity of infection (MOI) of 1. The cells were harvested, and internal luciferase activities were measured on day 0 though day 9 after adenovirus infection. Each assay was done in triplicate, and the value is displayed as a percentage of no treatment and as mean ± SD. An asterisk indicates a *P*-value of less than 0.05. (b) Dimethylthiazol carboxymethoxyphenyl sulfophenyl tetrazolium (MTS) assay of Huh7/pRep-Feo cells. Cells were infected with indicated recombinant adenoviruses at an MOI of 1. The assay was done at day 6 of infection. Error bars indicate mean + SD. (c) Northern blotting. The upper panel shows replicon RNA, and the lower panel shows beta-actin mRNA. (d) Western blotting. Total cell lysates were separated on NuPAGE gel, blotted and incubated with monoclonal anti-NS4A or anti-NS5A antibodies. The membrane was re-blotted with antibeta-actin antibodies. NT, untreated Huh7/pRep-Feo cells; Control, cells infected with AxshRNA-Control; HCV, cells treated with AxshRNA-HCV. In panels (b) and (c), cells were harvested on day 6 after adenovirus infection at an MOI of 1.

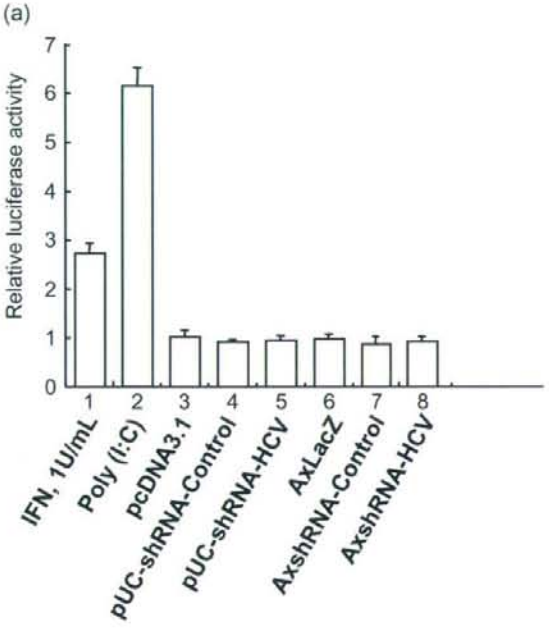

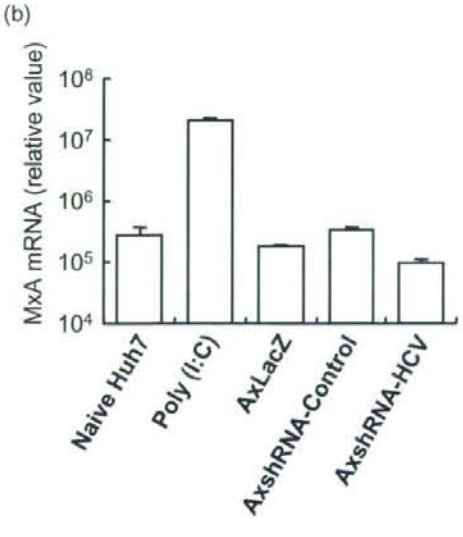

Figure 5 Interferon-stimulated gene responses by transfection of siRNA vectors. (a) Huh7 cells were seeded at 5×10^4 per well in 24-well plates on the day before transfection. As a positive control, 200 ng of pISRE-TA-Luc, or pTA-Luc, 1 ng of pRL-CMV, were transfected into a well using FuGENE-6 Transfection Reagent (Roche), and the cells were cultured with 1 U/mL of interferon (IFN) in the medium (lane 1). Lanes 3–5: 200 ng of pISRE-TA-Luc or pTA-Luc, and 1 ng of pRL-CMV were cotransfected with (lane2) 300 ng of poly (I : C), or 200 ng of plasmids (lane 3) pcDNA3.1, (lane 4) pUC19-shRNA-Control or (lane 5) pUC19-shRNA-HCV. Lanes 6–8: 200 ng of pISRE-TA-Luc or pTA-Luc, and 1 ng of pRL-CMV were transfected, and MOI = 1 of adenoviruses, (lane 6) AxLacZ, which expressed the beta-galactosidase (LacZ) gene under control of the chicken beta-actin (CAG) promoter as a control, (lane 7) AxshRNA-Control or (lane 8) AxshRNA-HCV were infected. Dual luciferase assays were performed at 48 h after transfection. The Fluc activity of each sample was normalized by the respective Rluc activity, and the respective pTA luciferase activity was subtracted from the pISRE luciferase activity. The experiment was done in triplicate, and the data are displayed as means + SD. (b) Huh7 cells were infected with indicated recombinant adenoviruses, AxLacZ, AxshRNA-Control and AxshRNA-HCV. RNA was extracted from each sample at day 6, and mRNA expression levels of an interferon-inducible MxA protein were quantified by the real-time RT-PCR analysis. Primers used were as follows: human MxA sense, 5′-CGA GGG AGA CAG GAC CAT CG-3′; human MxA antisense, 5′-TCT ATC AGG AAG AAC ATT TT-3′; human beta-actin sense, 5′-ACA ATG AAG ATC AAG ATC ATT GCT CCT CCT-3′; and human beta-actin antisense, 5′-TTT GCG GTG GAC GAT GGA GGG GCC GGA CTC-3′.

negative- or positive-control shRNA plasmids was transfected. (Fig. 5a). Similarly, the expression levels of an interferon-inducible MxA protein did not significantly change by transfection of shRNA-expression vectors (Fig. 5b). These results demonstrate that the shRNA used in the present study lack induction of the ISG responses both in the form of the expression plasmids and the adenovirus vectors.

Effect of siRNA and shRNA adenoviruses on HCV-JFH1 cell culture

The effects of HCV-targeted siRNA- and shRNA-expressing adenoviruses were confirmed by using HCV-JFH1 virus cell culture system. Transfection of the siRNA #331[14] into HCV-infected Huh7.5.1 cells resulted in substantial decrease of intracellular HCV RNA, while a control siRNA showed no effect (Fig. 6a). Similarly, infection of AxshRNA-HCV into Huh7.5.1/HCV-JFH1 cells specifically suppressed expression of HCV RNA (Fig. 6b).

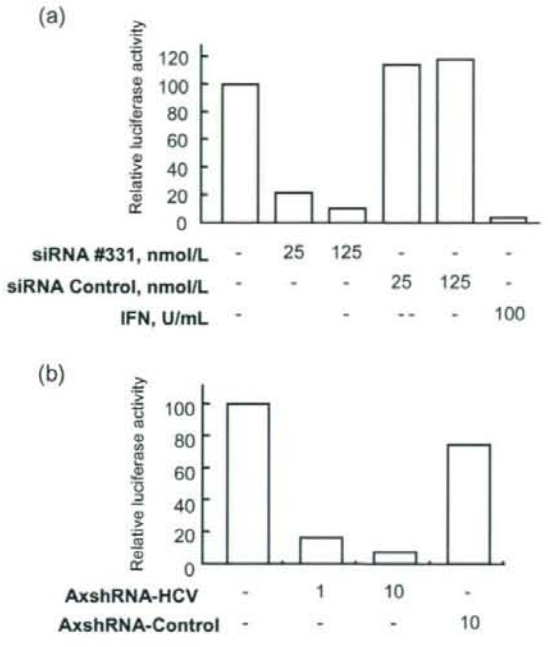

Figure 6 Effects of an siRNA and adenovirus expressing shRNA on HCV-JFH1 cell culture. (a) The siRNA #331, the siRNA-Control[14], (b) AxshRNA-HCV or AxshRNA-Control were, respectively, transfected or infected onto HV-JFH1-infected Huh7.5.1 cells. Seventy-two hours of the transfection or infection, expression level of HCV-RNA was quantified by real-time RT-PCR. The assays were repeated twice, and consistent results were obtained. IFN, recombinant interferon-alpha 2b.

Suppression of HCV-IRES-mediated translation *in vivo* by adenovirus expressing shRNA

The effects of the shRNA expression on the expression of the viral structural proteins *in vivo* were investigated using conditional HCV cDNA-transgenic mice, CN2-29.[28] Adenoviruses, AxshRNA-HCV, AxshRNA-Control or AxCAw1 were injected into CN2-29 mice in combination with AxCANCre, an adenovirus expressing *Cre* DNA recombinase. The mice were killed on the fourth day after the injection, and the hepatic expression of the HCV core protein was measured. The expressed amounts of the core protein were 143.0 ± 56.2 pg/mg and 108.5 ± 42.4 pg/mg in AxCAw1 and AxshRNA-Control-infected mice, respectively, and the expressed amount was significantly lower in mice injected with AxshRNA-HCV (28.7 ± 7.0 pg/mg, $P < 0.05$, Fig. 7a). Similarly, the induced expression of HCV core protein was not detectable by immunohistochemistry in AxshRNA-HCV infected liver tissue (Fig. 7c). Staining of a host cellular protein, albumin, was not obviously different between the liver infected with AxCAw1, AxshRNA-HCV and AxshRNA-Control (Fig. 7d). The expression levels of two ISG, IFN-beta and Mx1, in the liver tissue were not significantly different between individuals with and without injection of the adenovirus vectors (Fig. 7b). These results indicate specific shRNA silencing of HCV structural protein expression in the liver.

Discussion

The requirements to achieve a high efficiency using RNAi are: (i) selection of target sequences that are the most susceptible to RNAi; (ii) persistence of siRNA activity; and (iii) efficient *in vivo* delivery of siRNA to cells. We have used an shRNA sequence that was derived from a highly efficient siRNA (siRNA331), and constructed a DNA-based shRNA expression cassette that showed competitive effects with the synthetic siRNA (Fig. 2).[14] The shRNA-expression cassette does not only allow extended half-life of the RNAi, but also enables use of gene-delivery vectors, such as virus vectors. As shown in the results, a retrovirus vector expressing shRNA-HCV could stably transduce cells to express HCV-directed shRNA, and the cells acquired protection against HCV subgenomic replication (Fig. 3). An adenovirus vector expressing shRNA-HCV resulted in suppression of HCV subgenomic and protein expression by around three logs to almost background levels (Fig. 4). Consistent results were obtained by using an HCV cell culture (Fig. 6). More importantly, we have demonstrated *in-vivo* effects on viral protein expression in the liver using a conditional transgenic mouse model (Fig. 7). These results suggest that efficient delivery of siRNA could be effective against HCV infection *in vivo*.

An obstacle to applying siRNA technology to treat virus infections is that viruses are prone to mutate during their replication.[32] HCV continuously produces mutated viral strains to escape immune defense mechanisms. Even in a single patient, the circulating HCV population comprises a large number of closely related HCV sequence variants called quasispecies. Therefore, siRNA targeting the protein-coding sequence of the HCV genome, which have been reported by others,[15–19] may vary considerably among different HCV genotypes, and even among strains of the same genotype.[33] Our shRNA sequence targeted the 5′-UTR of HCV RNA, which is the most conserved region among various HCV isolates.[33] In addition, the structural constraints on the 5′-UTR, in terms of its requirement to direct internal ribosome entry and translation of viral proteins, might not permit the evolution of escape mutations. Our preliminary results have shown that the siRNA-HCV suppressed replication of an HCV genotype 2a replicon[34] to the same extent as the HCV 1b replicon.

Although the siRNA techniques rely on a high degree of specificity, several studies report siRNA-induced non-specific effect that may result from induction of ISG responses.[18,31] These effects may be mediated by activation of double-strand RNA-dependent protein kinase, toll-like receptor 3,[35] or possibly by a recently identified RNA helicase, RIG-I.[36] It remains to be determined whether these effects are generally induced by every siRNA construct. Sledz *et al.* have reported that transfection of two siRNA induced cellular interferon responses,[37] while Bridge *et al.* report that shRNA-expressing plasmids induced an interferon response but transfection of synthetic siRNA did not.[31] Speculatively, these effects on the interferon system might be construct dependent. Our shRNA-expression plasmids and adenoviruses did not activate ISG responses *in vitro* (Fig. 5a,b) or *in vivo* (Fig. 7b). We have preliminarily detected phosphorylated PKR (P-PKR) by western

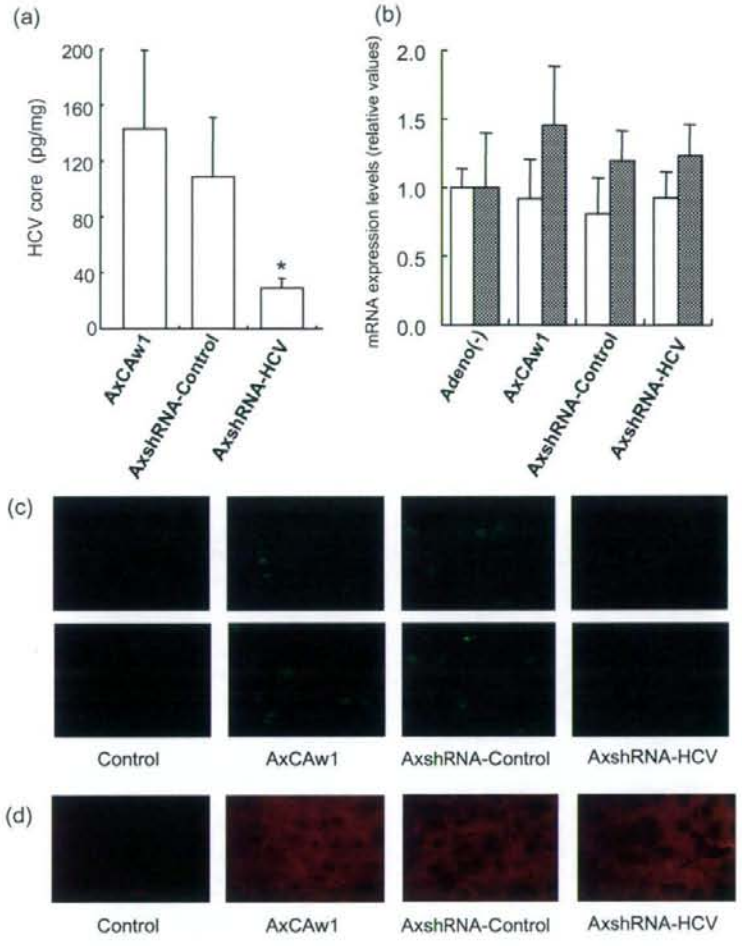

Figure 7 Effects of a recombinant adenovirus expressing shRNA on HCV core protein expression in CN2-29 transgenic mice. CN2-29 transgenic mice were administered with 1×10^8 PFU of AxCANCre combined with 6.7×10^8 PFU of AxshRNA-HCV, AxshRNA or AxCAw1. The mice were killed on day 4 after injection. (a) Quantification of HCV core protein in liver. Liver tissues were homogenized and used to determine the amount of HCV core protein. Each assay was done in triplicate, and the values are displayed as mean ± SD. Asterisk indicates *P*-value of less than 0.05. (b) Expression levels of mouse interferon-beta (white bars) and Mx1 (shaded bars) mRNA in the mouse liver tissue were quantified by the real-time RT-PCR analyses. Primers used were as follows: mouse interferon-beta sense, 5′-ACA GCC CTC TCC ATC AAC TA-3′; mouse interferon-beta antisense, 5′-CCC TCC AGT AAT AGC TCT TC-3′; mouse Mx1 sense, 5′-AGG AGT GGA GAG GCA AAG TC-3′; mouse Mx1 antisense, 5′-CAC ATT GCT GGG GAC TAC CA-3′; mouse beta-actin sense, 5′-ACT CCT ATG TGG GTG ACG AG-3′; mouse beta-actin antisense, 5′-ATA GCC CTC GTA GAT GGG CA-3′. Adeno (-) denotes mice without adenovirus administration. (c) Immunofluorescence microscopy of HCV core protein in the liver tissue. Liver sections of mice were stained using rabbit anticore polyclonal antibody and normal rabbit IgG as a negative control. The upper photographs were obtained at 400× magnification, and the lower photographs were at 1000×. (d) Immunofluorescence microscopy of albumin in liver. Liver sections from the mice were fixed and stained using rabbit antialbumin antibody and normal rabbit IgG as a negative control.

blotting, and found no apparent increase of P-PKR (data not shown). These results indicate that these target sequences and structures are of sufficient specificity to silence the target gene without eliciting non-specific interferon responses.

Beside the canonical action of siRNA, a sequence-specific cleavage of target mRNA, the siRNA could act as a micro-RNA that suppresses translational initiation of mRNA,[38] or it could mediate transcriptional gene silencing.[39] Regarding our *in-vivo* experiments, it was difficult to differentially analyze the effect of siRNA at individual sites of action because post-translational effect of siRNA concomitantly destabilizes target mRNA, which leads to apparent decrease of mRNA transcripts.

Efficiency and safety of gene transfer methods are the key determinants of the clinical success of gene therapy and an unresolved problem. There are several reports of delivery of siRNA or siRNA-expression vectors to cells *in vivo*;[12,40,41] however, gene delivery methods that are safe enough to apply to clinical therapeutics are currently under development. Adenovirus vectors are one of the most commonly used carriers for human gene therapies.[42–44] Our present results demonstrate that the adenoviral delivery of shRNA is effective in blocking HCV replication *in vitro* and virus protein expression *in vivo*. Adenovirus vectors have several advantages of efficient delivery of transgene both *in vitro* and *in vivo* and natural hepatotropism when administered *in vivo*. The AxshRNA-HCV specifically blocked expression of HCV structural proteins in a conditional transgenic mouse expressing those proteins. The current adenovirus vectors may cause inflammatory reactions in the target organ,[45] however, and produce neutralizing antibodies which make repeated administration difficult. These problems may be overcome by the improved constructs of virus vectors with attenuated immunogenicity or by the development of non-viral carriers for gene delivery.[46]

In conclusion, our results demonstrate the effectiveness and feasibility of the siRNA expression system. The efficiency of adenovirus expressing shRNA that target HCV suggests that delivery and expression of siRNA in hepatocytes may eliminate the virus and that this RNA-targeting approach might provide a potentially effective future therapeutic option for HCV infection.

Acknowledgments

This study was supported by grants from Japan Society for the Promotion of Science, 15590629 and 16590580, and partly supported by a grant from the Viral Hepatitis Research Foundation of Japan.

References

1 Alter MJ. Epidemiology of hepatitis C. *Hepatology* 1997; **26**: 62S–65S.
2 Hadziyannis SJ, Sette H Jr, Morgan TR *et al.* Peginterferon-alpha2a and ribavirin combination therapy in chronic hepatitis C: a randomized study of treatment duration and ribavirin dose. *Ann. Intern. Med.* 2004; **140**: 346–55.
3 Fire A, Xu S, Montgomery M, Kostas S, Driver S, Mello C. Potent and specific genetic interference by double-stranded RNA in Caenorhabditis elegans. *Nature* 1998; **19**: 806–11.
4 Elbashir SM, Harborth J, Lendeckel W, Yalcin A, Weber K, Tuschl T. Duplexes of 21-nucleotide RNAs mediate RNA interference in cultured mammalian cells. *Nature* 2001; **411**: 494–8.
5 Coburn GA, Cullen BR. Potent and specific inhibition of human immunodeficiency virus type 1 replication by RNA interference. *J. Virol.* 2002; **76**: 9225–31.
6 Jacque JM, Triques K, Stevenson M. Modulation of HIV-1 replication by RNA interference. *Nature* 2002; **418**: 435–8.
7 Gitlin L, Karelsky S, Andino R. Short interfering RNA confers intracellular antiviral immunity in human cells. *Nature* 2002; **418**: 430–4.
8 Ge Q, Filip L, Bai A, Nguyen T, Eisen HN, Chen J. Inhibition of influenza virus production in virus-infected mice by RNA interference. *Proc. Natl. Acad. Sci. USA* 2004; **101**: 8676–81.
9 Wang C, Pflugheber J, Sumpter R Jr *et al.* Alpha interferon induces distinct translational control programs to suppress hepatitis C virus RNA replication. *J. Virol.* 2003; **77**: 3898–912.
10 Klein C, Bock CT, Wedemeyer H *et al.* Inhibition of hepatitis B virus replication in vivo by nucleoside analogues and siRNA. *Gastroenterology* 2003; **125**: 9–18.
11 Konishi M, Wu CH, Wu GY. Inhibition of HBV replication by siRNA in a stable HBV-producing cell line. *Hepatology* 2003; **38**: 842–50.
12 McCaffrey AP, Meuse L, Pham TT, Conklin DS, Hannon GJ, Kay MA. RNA interference in adult mice. *Nature* 2002; **418**: 38–9.
13 Shlomai A, Shaul Y. Inhibition of hepatitis B virus expression and replication by RNA interference. *Hepatology* 2003; **37**: 764–70.
14 Yokota T, Sakamoto N, Enomoto N *et al.* Inhibition of intracellular hepatitis C virus replication by synthetic and vector-derived small interfering RNAs. *EMBO Rep.* 2003; **4**: 602–8.
15 Kapadia SB, Brideau-Andersen A, Chisari FV. Interference of hepatitis C virus RNA replication by short interfering RNAs. *Proc. Natl. Acad. Sci. USA* 2003; **100**: 2014–18.
16 Kronke J, Kittler R, Buchholz F *et al.* Alternative approaches for efficient inhibition of hepatitis C virus RNA replication by small interfering RNAs. *J. Virol.* 2004; **78**: 3436–46.
17 Randall G, Grakoui A, Rice CM. Clearance of replicating hepatitis C virus replicon RNAs in cell culture by small interfering RNAs. *Proc. Natl. Acad. Sci. USA* 2003; **100**: 235–40.
18 Seo MY, Abrignani S, Houghton M, Han JH. Letter to the editor: small interfering RNA-mediated inhibition of hepatitis C virus replication in the human hepatoma cell line Huh-7. *J. Virol.* 2003; **77**: 810–12.
19 Wilson JA, Jayasena S, Khvorova A *et al.* RNA interference blocks gene expression and RNA synthesis from hepatitis C replicons propagated in human liver cells. *Proc. Natl. Acad. Sci. USA* 2003; **100**: 2783–8.
20 Guo JT, Bichko VV, Seeger C. Effect of alpha interferon on the hepatitis C virus replicon. *J. Virol.* 2001; **75**: 8516–23.
21 Tanabe Y, Sakamoto N, Enomoto N *et al.* Synergistic inhibition of intracellular hepatitis C virus replication by combination of ribavirin and interferon-alpha. *J. Infect. Dis.* 2004; **189**: 1129–39.
22 Maekawa S, Enomoto N, Sakamoto N *et al.* Introduction of NS5A mutations enables subgenomic HCV-replicon derived from chimpanzee-infectious HC-J4 isolate to replicate efficiently in Huh-7 cells. *J. Viral. Hepat.* 2004; **11**: 394–403.
23 Miyagishi M, Sumimoto H, Miyoshi H, Kawakami Y, Taira K. Optimization of an siRNA-expression system with an improved hairpin and its significant suppressive effects in mammalian cells. *J. Gene Med.* 2004; **6**: 715–23.
24 Li Y, Yokota T, Matsumura R, Taira K, Mizusawa H. Sequence-dependent and independent inhibition specific for mutant ataxin-3 by small interfering RNA. *Ann. Neurol.* 2004; **56**: 124–9.
25 Kanazawa N, Kurosaki M, Sakamoto N *et al.* Regulation of hepatitis C virus replication by interferon regulatory factor-1. *J. Virol.* 2004; **78**: 9713–20.
26 Wakita T, Pietschmann T, Kato T *et al.* Production of infectious hepatitis C virus in tissue culture from a cloned viral genome. *Nat. Med.* 2005; **11**: 791–6.
27 Zhong J, Gastaminza P, Cheng G *et al.* Robust hepatitis C virus infection in vitro. *Proc. Natl. Acad. Sci. USA* 2005; **102**: 9294–9.
28 Wakita T, Taya C, Katsume A *et al.* Efficient conditional transgene expression in hepatitis C virus cDNA transgenic mice mediated by the Cre/loxP system. *J. Biol. Chem.* 1998; **273**: 9001–6.
29 Kashiwakuma T, Hasegawa A, Kajita T *et al.* Detection of hepatitis C virus specific core protein in serum of patients by a sensitive fluorescence enzyme immunoassay (FEIA). *J. Immunol. Methods* 1996; **28**: 79–89.

30 Baglioni C, Nilsen TW. Mechanisms of antiviral action of interferon. *Interferon* 1983; **5**: 23–42.
31 Bridge A, Pebernard S, Ducraux A, Nicoulaz A, Iggo R. Induction of an interferon response by RNAi vectors in mammalian cells. *Nat. Genet.* 2003; **34**: 263–4.
32 Carmichael GG. Silencing viruses with RNA. *Nature* 2002; **418**: 379–80.
33 Okamoto H, Okada S, Sugiyama Y *et al.* Nucleotide sequence of the genomic RNA of hepatitis C virus isolated from a human carrier: comparison with reported isolates for conserved and divergent regions. *J. Gen. Virol.* 1991; **72**: 2697–704.
34 Kato T, Date T, Miyamoto M *et al.* Efficient replication of the genotype 2a hepatitis C virus subgenomic replicon. *Gastroenterology* 2003; **125**: 1808–17.
35 Alexopoulou L, Holt AC, Medzhitov R, Flavell RA. Recognition of double-stranded RNA and activation of NF-kB by Toll-like receptor 3. *Nature* 2001; **413**: 732–8.
36 Yoneyama M, Kikuchi M, Natsukawa T *et al.* The RNA helicase RIG-I has an essential function in double-stranded RNA-induced innate antiviral responses. *Nat. Immunol.* 2004; **5**: 730–7.
37 Sledz C, Holko M, de Veer M, Silverman R, Williams, B. Activation of the interferon system by short-interfering RNAs. *Nat. Cell. Biol.* 2003; **5**: 834–9.
38 Doench JG, Petersen CP, Sharp PA. siRNAs can function as miRNAs. *Genes Dev.* 2003; **17**: 438–42.
39 Morris KV. siRNA-mediated transcriptional gene silencing: the potential mechanism and a possible role in the histone code. *Cell. Mol. Life Sci.* 2005; **62**: 3057–66.
40 Xia H, Mao Q, Paulson HL, Davidson BL. siRNA-mediated gene silencing in vitro and in vivo. *Nat. Biotechnol.* 2002; **20**: 1006–10.
41 Zender L, Hutker S, Liedtke C *et al.* Caspase 8 small interfering RNA prevents acute liver failure in mice. *Proc. Natl. Acad. Sci. USA* 2003; **100**: 7797–802.
42 Akli S, Caillaud C, Vigne E *et al.* Transfer of a foreign gene into the brain using adenovirus vectors. *Nat. Genet.* 1993; **3**: 224–8.
43 Bajocchi G, Feldman SH, Crystal RG, Mastrangeli A. Direct in vivo gene transfer to ependymal cells in the central nervous system using recombinant adenovirus vectors. *Nat. Genet.* 1993; **3**: 229–34.
44 Davidson BL, Allen ED, Kozarsky KF, Wilson JM, Roessler BJ. A model system for in vivo gene transfer into the central nervous system using an adenoviral vector. *Nat. Genet.* 1993; **3**: 219–23.
45 Yang Y, Wilson JM. Clearance of adenovirus-infected hepatocytes by MHC class I-restricted CD4+ CTLs in vivo. *J. Immunol.* 1995; **155**: 2564–70.
46 Fleury S, Driscoll R, Simeoni E *et al.* Helper-dependent adenovirus vectors devoid of all viral genes cause less myocardial inflammation compared with first-generation adenovirus vectors. *Basic Res. Cardiol.* 2004; **99**: 247–56.

Potential Relevance of Cytoplasmic Viral Sensors and Related Regulators Involving Innate Immunity in Antiviral Response

YASUHIRO ASAHINA,* NAMIKI IZUMI,* ITSUKO HIRAYAMA,* TOMOHIRO TANAKA,* MITSUAKI SATO,*,‡ YUTAKA YASUI,* NOBUTOSHI KOMATSU,*,‡ NAOKI UMEDA,* TAKANORI HOSOKAWA,* KEN UEDA,* KAORU TSUCHIYA,* HIROYUKI NAKANISHI,* JUN ITAKURA,* MASAYUKI KUROSAKI,* NOBUYUKI ENOMOTO,‡ MEGUMI TASAKA,§ NAOYA SAKAMOTO,§ and SHOZO MIYAKE*

*Department of Gastroenterology and Hepatology, Musashino Red Cross Hospital, Tokyo; ‡First Department of Internal Medicine, Faculty of Medicine, University of Yamanashi, Yamanashi; and §Department of Gastroenterology and Hepatology, Tokyo Medical and Dental University, Tokyo, Japan

Background & Aims: **Clinical significance of molecules involving innate immunity in treatment response remains unclear. The aim is to elucidate the mechanisms underlying resistance to antiviral therapy and predictive usefulness of gene quantification in chronic hepatitis C (CH-C).** ***Methods:*** **We conducted a human study in 74 CH-C patients treated with pegylated interferon α-2b and ribavirin and 5 nonviral control patients. Expression of viral sensors, adaptor molecule, related ubiquitin E3-ligase, and modulators were quantified.** ***Results:*** **Hepatic RIG-I, MDA5, LGP2, ISG15, and USP18 in CH-C patients were up-regulated at 2- to 8-fold compared with non-hepatitis C virus patients with a relatively constitutive Cardif. Hepatic RIG-I, MDA5, and LGP2 were significantly up-regulated in nonvirologic responders (NVR) compared with transient (TR) or sustained virologic responders (SVR). Cardif and RNF125 were negatively correlated with RIG-I and significantly suppressed in NVR. Differences among clinical responses in RIG-I/Cardif and RIG-I/RNF125 ratios were conspicuous (NVR/TR/SVR = 1.3:0.6:0.4 and 2.3:1.3:0.8, respectively). Like viral sensors, ISG15 and USP18 were significantly up-regulated in NVR (4-fold and 2.3-fold, respectively). Multivariate and receiver operator characteristic analyses revealed higher RIG-I/Cardif ratio, ISG15, and USP18 predicted NVR. Lower Cardif in NVR was confirmed by its protein level in Western blot. Also, transcriptional responses in peripheral blood mononuclear cells to the therapy were rapid and strong except for Cardif in not only a positive (RIG-I, ISG15, and USP18) but also in a negative regulatory manner (RNF125).** ***Conclusions:*** **NVR may have adopted a different equilibrium in their innate immune response. High RIG-I/Cardif and RIG-I/RNF125 ratios and ISG15 and USP18 are useful in identifying NVR.**

Infection with hepatitis C virus (HCV) is a common cause of chronic hepatitis, which progresses to cirrhosis and hepatocellular carcinoma in many patients.[1] Although combination therapy with pegylated interferon (PEG-IFN) α and ribavirin is now established as the standard treatment for chronic HCV infection genotype 1b, the sustained virologic response rate in these patients is still around 50%.[2–4] Moreover, physicians have also found that 20% of patients are nonvirologic responders (NVR; those whose HCV-RNA does not become negative during 48 weeks of combination therapy).[5] Prediction of NVR status is of clinical importance because these patients have no chance of achieving a sustained virologic response even after prolonged combination therapy.[6] However, mechanisms involving resistance to PEG-IFN-α and ribavirin have not been fully elucidated, and it is difficult to predict treatment responses before initiation of PEG-IFN-α and ribavirin combination therapy.

In vitro studies have suggested that an innate immune response in viral infection is an essential part of the host antiviral defense system.[7] HCV evades the host immune response through a complex combination of processes that include signaling interference, effector modulation, and continual viral genetic variation.[8] We hypothesized that liver tissue would show a consistent difference between responders and nonresponders in expression levels of the gene involved in innate immunity and IFN signal transduction. These differences could be used to predict treatment outcomes.

The retinoic acid–inducible gene I (RIG-I), a cytoplasmic RNA helicase, and the related melanoma differentia-

Abbreviations used in this paper: CARD, Caspase-recruiting domain; Cardif, caspase-recruiting domain adaptor inducing IFN-β; G3PDH, glyceraldehyde-3-phosphate dehydrogenase; HCV, hepatitis C virus; IPS-1, IFN-β promoter stimulator I; ISG15, IFN-stimulated gene 15; PEG-IFN, pegylated interferon; MDA5, melanoma differentiation associated gene 5; MAVS, mitochondrial antiviral signaling protein; NVR, nonvirologic responders; PBMC, peripheral blood mononuclear cell; RIG-I, retinoic acid-inducible gene I; RNF125, ring-finger protein 125; ROC, receiver operator characteristic; SVR, sustained viral responder; TR, transient responder; UBP43, ubiquitin-specific protease 43; USP18, ubiquitin-specific protease 18; VISA, virus-induced signaling adaptor.

0016-5085/08/$34.00
doi:10.1053/j.gastro.2008.02.019

Table 1. Patient Characteristics at Baseline According to Final Virologic Response

	SVR n = 30	TR n = 24	NVR n = 20	*P* value
Age (*y*)	52 ± 13	60 ± 8.7	60 ± 10	.04[a]
Female % (M/F)	47% (16/14)	63% (9/15)	60% (8/12)	.5[b]
Naïve & Relapser[c]/Non-responder[c]	26/4	20/4	14/6	.3[b]
BMI	24.6 ± 3.0	24.9 ± 4.4	24.0 ± 2.1	.6[a]
ALT (*IU/L*)	75 ± 57	65 ± 35	68 ± 41	1.0[a]
Hemoglobin (*g/dL*)	14.3 ± 1.6	14.1 ± 1.1	14.5 ± 1.7	.6[a]
Platelet count ($\times 10^3/\mu L$)	182 ± 62	169 ± 48	140 ± 39	.04[a]
Liver histology				
A1/A2/A3	19/8/3	14/8/1	10/10/0	.3[b]
F1/F2/F3	14/9/7	11/7/5	7/5/8	.7[b]
Viral load ($\times 10^6$ *IU/mL*)	1.6 ± 1.2	1.8 ± 1.1	1.6 ± 1.1	.8[a]
Viral decline rate ($\log_{10}$/day)				
First phase	2.1 ± 0.9	1.5 ± 0.6	0.7 ± 0.5	<.0001[a]
Second phase	0.05 ± 0.05	0.04 ± 0.02	0.006 ± 0.008	<.0001[a]

ALT, alanine aminotransferase; BMI, body mass index.
[a]*P* values were determined by Kruskal–Wallis test.
[b]*P* values were determined by chi-square test.
[c]Response to previous IFN treatment.

tion-associated gene 5 (MDA5) play essential roles in initiating the host antiviral response by detecting intracellular viral dsRNA.[9,10] Caspase-recruiting domain (CARD) adaptor inducing IFN-β (Cardif), also called IFN-β promoter stimulator 1 (IPS-1), mitochondrial antiviral signaling protein (MAVS), and virus-induced signaling adaptor (VISA), is an adaptor molecule. Cardif connects RIG-I sensing to downstream signaling, resulting in IFN-β gene activation.[11–14] On the other hand, RIG-I sensing has been shown to be negatively regulated in a dominant-negative manner by LGP2,[10,15] a helicase related to RIG-I and MDA5 lacking CARD. Interestingly, the ubiquitin ligase ring-finger protein 125 (RNF125) has been recently shown to conjugate ubiquitin to RIG-I, MDA5 as well as Cardif, which results in suppressing the functions of these proteins.[16] Furthermore, these molecules are conjugated (ISGylated) by IFN-stimulated gene 15 (ISG15), a ubiquitin-like protein,[17] and ISG15 is specifically removed from ISGylated protein by ubiquitin-specific protease 18 (USP18), also called ubiquitin-specific protease 43 (UBP43).[18,19] Moreover, the NS3/4A protease of HCV specifically cleaves Cardif as part of its immune evasion strategy.[11,20] Therefore, the RIG-I/Cardif system and its regulatory systems have essential key functions in the innate antiviral response (see Supplementary Figure 1 online at www.gastrojournal.org). However, the clinical significance of these innate immune systems, especially in relevance to the treatment response, is unclear because findings in this field have been mainly obtained by in vitro experiments using cell lines.

The aims of this study were to elucidate the mechanisms underlying resistance to antiviral therapy in the clinical setting and to determine whether quantification of transcripts of positive and negative cytoplasmic viral sensors and related regulatory molecules involving innate immune system is useful in predicting responses to PEG-IFN-α and ribavirin combination therapy.

Patients and Methods

Patients

Among patients with biopsy-proven chronic hepatitis C hospitalized at the Musashino Red Cross Hospital, 74 patients of HCV genotype 1b with a high viral load (>100,000 IU/mL by Amplicor-HCV Monitor Assay; Roche Molecular Diagnostics Co, Tokyo, Japan) were included in the present study (Table 1). Patients with cirrhosis, autoimmune hepatitis, or alcoholic liver injury were excluded. No patient was positive for hepatitis B virus–associated antigen/antibody or anti–human immunodeficiency virus antibody. No patient received immunomodulatory therapy prior to the enrollment. Written informed consent was obtained from all the patients, and this study was approved by the Ethical Committee of Musashino Red Cross Hospital in accordance with the Helsinki Declaration. Five patients with nonviral liver disease (2 had autoimmune hepatitis and 3 had primary biliary cirrhosis) were included in the present study as controls.

Treatment Protocol

The patients were treated for 48 weeks with subcutaneous injections of PEG-IFN-α-2b (PegIntron; Schering-Plough Corporation, Kenilworth, NJ) at a dose of 1.5 $\mu g \cdot kg^{-1} \cdot week^{-1}$. Ribavirin (Rebetol; Schering-Plough Corporation) was administered concomitantly over the 48-week period, given orally twice daily at a total daily dose of 600 mg for the patients who weighed less than 60 kg and 800 mg for the patients who weighed between 60 and 80 kg. The dose of PEG-IFN-α-2b was reduced to 0.75 $\mu g \cdot kg^{-1} \cdot week^{-1}$ when either the neutrophil count was $<750/mm^3$ or the platelet count was $<80 \times 10^3/mm^3$. The dose of ribavirin was reduced to 600 mg/day when the hemoglobin concentration decreased to <10 g/dL.

Measurement of Gene Expression in the Liver

Liver biopsy was performed immediately before starting the therapy. After extraction of total RNA from liver biopsy specimens, the messenger RNA (mRNA) expression of positive and negative cytoplasmic viral sensors (RIG-I, MDA5, and LGP2), the adaptor molecule (Cardif), related ubiquitin E3-ligase (RNF125), and the modulators of these molecules (ISG15 and USP18) was quantified by real-time quantitative polymerase chain reaction (PCR) using primers specific for target genes. In brief, total RNA was extracted by the acid-guanidinium-phenol-chloroform method using Isogen (Nippon Gene Co Ltd, Toyama, Japan) from the liver biopsy specimen, which was 0.2–0.4 cm in length and 13 gauge in diameter. Complementary DNA (cDNA) was transcribed from 2 μg total RNA template in a 140-μL reaction mixture using a SYBR RT-PCR Kit (Takara Bio Co Ltd, Otsu, Japan) with random hexamer. Real-time quantitative PCR was performed using Smart Cycler version II (Takara Bio Co Ltd) with the SYBR RT-PCR Kit (Takara Bio Co Ltd) according to the manufacturer's instructions, and intercalating SYBR Green I (Molecular Probes Inc, Eugene, Oregon) was detected. Assays were performed in duplicate, and the expression levels of target genes were normalized to expression of the glyceraldehyde-3-phosphate dehydrogenase (G3PDH) gene and hydroxymethylbilane synthase, which is stable in the liver, as quantified using real-time quantitative PCR as internal controls. For accurate normalization, a set of 2 housekeeping genes was used in the present study. Sequences of primer sets were as follows: RIG-I: 5′-AAAGCATGCATGGTGTTCCAGA-3′, 5′-TCATTCGTGCATGCTCACTGATAA-3′; MDA5: 5′-ACATAACAGCAACATGGGCAGTG-3′, 5′-TTTGGTAAGGCCTGAGCTGGAG-3′; LGP2: 5′-ACAGCCTTGCAAACAGTACAACCTC-3′, 5′-GTCCCAAATTTCCGGCTCAAC-3′; Cardif: 5′-GGTGCCATCCAAAGTGCCTACTA-3′, 5′-CAGCACGCCAGGCTTACTCA-3′; RNF125: 5′-AGGGCACATATTCGGACTTGTCA-3′, 5′-CGGGTATTAAACGGCAAAGTGG-3′; ISG15: 5′-AGCGAACTCATCTTTGCCAGTACA-3′, 5′-CAGCTCTGACACCGACATGGA-3′; USP18: 5′-TGGTTCTGCTTCAATGACTCCAATA-3′, 5′-TTTGGGCATTTCCATTAGCACTC-3′; GAPDH: 5′-GCACCGTCAAGGCTGAGAAC-3′, 5′-TGGTGGTGAAGACGCCAGT-3′. hydroxymethylbilane synthase: 5′-AAGCGGAGCCATGTCTGGTAAC-3′, 5′-GTACCCACGCGAATCACTCTCA-3′.

Sequential Measurement of Gene Expression in Peripheral Blood Mononuclear Cells Before and During Therapy

To understand transcriptional response of the genes to PEG-IFN-α-2b and ribavirin therapy, serial expression of RIG-I, RNF125, Cardif, ISG15, and USP18 were determined before and during treatment in peripheral blood mononuclear cells (PBMC) in 14 patients (7 were sustained viral responders [SVR] and 7 were NVR). PBMC was obtained from whole blood samples collected before and at 4, 8, 24, 48, and 168 hours after the initiation of PEG-IFN-α-2b and ribavirin combination therapy. After extraction of total RNA from the PBMC, the expression of mRNA was quantified at each specified time point using real-time quantitative PCR as described above. Gene expression levels at each time point during treatment were calculated relative to baseline expression levels measured prior to IFN treatment.

Western Blotting

Western blotting was carried out in 9 patients (5 were SVR and 4 were NVR) and 3 non-HCV control subjects as described previously.[21] Liver biopsy specimen of ~10 mg was homogenized in 100 μL Complete Lysis-M (Roche Applied Science, Penzberg, Germany). Twenty micrograms of the homogenates were separated by SDS-PAGE and blotted onto a polyvinylidene difluoride Western blotting membrane. The membrane was incubated with the primary antibodies followed by a peroxidase-labeled anti-IgG antibody and visualized by chemiluminescence using the ECL Western blotting Analysis System (Amersham Biosciences, Buckinghamshire, United Kingdom). The anti-VISA mouse monoclonal antibody (BioDesign, Saco, ME) and anti-β-actin antibody (Sigma Chemical Co, St. Louis, MO) were used.

HCV Dynamics in Serum

To analyze the viral dynamics, HCV RNA was quantified just before and at 4, 8, and 24 hours and 2, 7, 14, 28, 56, and 84 days after the initiation of PEG-IFN-α-2b and ribavirin combination therapy, using real-time detection PCR, as reported previously.[22] For each patient, the viral decline curve was plotted on a semilogarithmic scale, and the slopes of the exponential viral declines were calculated for each viral decline phase with a straight-line fit of the data.

Definitions of Response to Therapy

A patient negative for serum HCV RNA during the first 6 months after the completion of PEG-IFN-α-2b and ribavirin combination therapy was defined as an SVR, and a patient for whom HCV RNA became negative at the end of therapy and reappeared after completion of therapy was defined as a transient responder (TR). A patient who was positive for HCV RNA even during the course of therapy was defined as an NVR. HCV RNA was determined with the Amplicor qualitative assay (Roche Molecular Diagnostics Co, Tokyo, Japan). The detection sensitivity of this assay is approximately 50 IU/mL.

Statistical Analysis

Categorical data were compared by the χ^2 test and Fisher exact test. Distributions of continuous variables were analyzed by Mann–Whitney U test for 2 groups. Kruskal–Wallis test was used for multiple group comparisons. All tests of significance were 2-tailed, and P values $< .05$ were considered statistically significant.

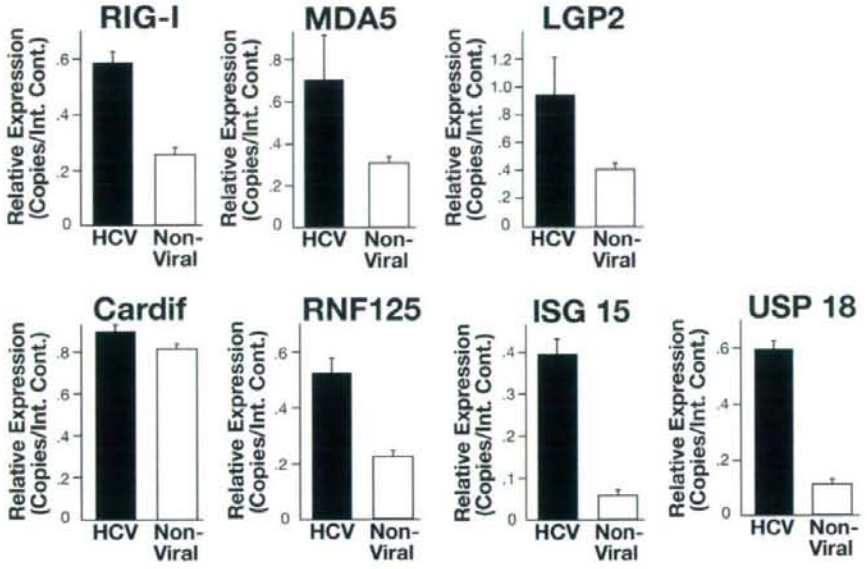

Figure 1. Comparison of hepatic gene expression levels between chronic hepatitis C patients (n = 74) and nonviral liver disease patients (n = 5). Expression levels of RIG-I, MDA5, LGP2, Cardif, RNF125, ISG15, and USP18 are shown. *Error bars* indicate the standard error. Upon HCV infection, expression of these genes except Cardif was stimulated. The *P* values determined by Mann–Whitney *U* test between 2 groups were as follows: RIG-I, *P* .02; MDA5, *P* .01; LGP2, *P* .005; Cardif, *P* .7; RNF125, *P* .06; ISG15, *P* .007; USP18, *P* .004.

Results

Patient Characteristics

According to the final virologic response, patients were classified into 3 groups: 30 were SVR, 24 were TR, and the remaining 20 were NVR, as shown in Table 1. Viral decline rates in NVR were significantly lower in both the first and second phases of HCV dynamics. It should be noted that most NVR patients exhibited no second-phase viral decline.

Data on factors that were available before starting the treatment were compared according to virologic response by univariate analysis. As shown in Table 1, only age and platelet count were associated with viral response, and no other clinical factors were predictive of NVR before initiation of the therapy.

Gene Expression Involving Innate Immunity in the Liver

First, we compared basal hepatic gene expression between the chronic hepatitis C patients (n = 74) and the nonviral liver disease patients (n = 5). As shown in Figure 1, levels of RIG-I, MDA5, LGP2, ISG15, and USP18 expression were significantly higher in the chronic hepatitis C patients than in the nonviral liver disease patients. However, there was no significant difference in levels of Cardif expression between the chronic hepatitis C and nonviral-related liver disease patients.

Next, to assess the relationship between baseline hepatic gene expression and treatment efficacy, levels of gene expression were compared based on the final virologic response. As shown in Figure 2, the hepatic expression levels of RIG-I, MDA5, and LGP2 were significantly higher in NVR than in SVR and TR. In marked contrast, hepatic Cardif expression was significantly lower in the NVR group. The hepatic expression of RNF125, which is specific E3-ubiquitin ligase for RIG-I, MDA5, and Cardif, was also significantly lower in the NVR group. Because negative correlation was found between RIG-I and Cardif or RNF125 expression, we calculated the ratio of RIG-I to Cardif or RNF125 expression levels. As shown in Figure 2, the difference among the groups was conspicuous when comparison was made with the RIG-I/Cardif ratio or RIG-I/RNF125 ratio. Moreover, the RIG-I/Cardif expression ratio before treatment was negatively and significantly correlated with the exponential viral decline rate in both the first and the second phases of HCV dynamics (first phase, $r = -0.4$, $P < .0005$; second phase, $r = -0.5$, $P < .0001$). Similar correlation was found between RIG-I/RNF125 ratio and viral decline rate (first phase, $r = -0.4$, $P = .004$; second phase, $r = -0.2$, $P = .09$, data not shown).

Like RIG-I and MDA5, intrahepatic expression levels of ISG15 and USP18 were significantly higher in NVR than in SVR and TR (Figure 2). When we assessed the correlation of these 2 genes in individual patients, we found a strong and significant correlation between ISG15 and USP18 ($r^2 = 0.88$, $P < .0001$). Levels of ISG15 and USP18 expression before treatment were negatively correlated with the exponential viral decline rates calculated from

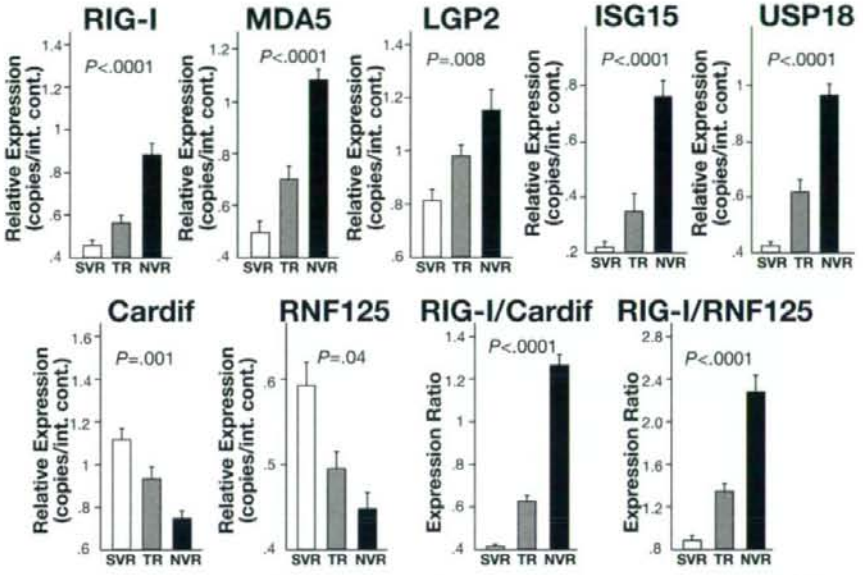

Figure 2. Comparison of hepatic gene expression levels according to final virologic outcome. Expression levels of RIG-I, MDA5, LGP2, ISG15, USP18, Cardif, RNF125, RIG-I/Cardif ratio, and RIG-I/RNF125 ratio are shown. *Open columns* indicate SVR (n = 30), *shaded columns* indicate TR (n = 24), and *solid columns* indicate NVR (n = 20). *Error bars* indicate the standard error. The *P* values were analyzed by the Kruskal–Wallis test.

the first and the second phases of HCV dynamics (ISG15, first phase, $r = -0.5$, $P < .0001$; ISG15, second phase, $r = -0.3$, $P = .02$; USP18, first phase, $r = -0.5$, $P < .0001$; USP18, second phase, $r = -0.3$, $P = .01$).

Receiver Operator Characteristic Analysis

To determine the usefulness of these gene quantifications as predictors, receiver operator characteristic (ROC) analysis was conducted (Figure 3). The area under the ROC curve for the RIG-I/Cardif ratio, ISG15, and USP18 was 0.91, 0.90, and 0.91, respectively, suggesting that quantification of these gene transcripts is of use for the prediction of NVR (Table 2). In addition, this analysis also suggested that RIG-I/Cardif ratio would be more specific for prediction of NVR, whereas ISG15 and USP18 would be more sensitive (Table 2).

Multivariate Analysis

Multivariate analysis for factors that were available before initiating therapy indicated that a higher ratio of RIG-I/Cardif and higher expression of ISG15 were independent factors that were associated with NVR (Table 3). In this analysis, USP18 was excluded because of its strong correlation with ISG15.

Protein Levels of Cardif in the Liver

Because hepatic expression of Cardif mRNA was significantly lower in NVR patients than in SVR patients,

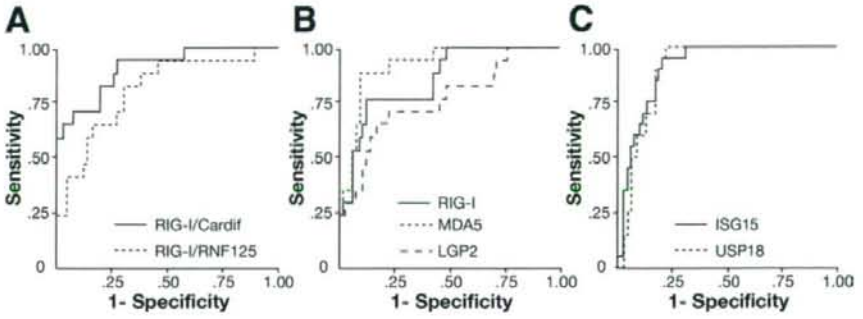

Figure 3. Receiver operator characteristic (ROC) curve for prediction of nonvirologic response. ROC curves were generated to compare (*A*) RIG-I/Cardif ratio (*solid line*) and RIG-I/RNF125 ratio (*shaded line*); (*B*) RIG-I (*solid line*), MDA5 (*shaded line*), and LGP2 (*dotted line*); and (*C*) ISG15 (*solid line*) and USP18 (*shaded line*).